CFD Simulation of Thermal Runaway Scenario in Styrene Polymerization Reaction

Yating Chen [a], Jiajia Jiang [b *]

Jiangsu Key Laboratory of Hazardous Chemicals Safety and Control, College of Safety Science and Engineering, Nanjing Tech University, Nanjing, 211816, China

[a] 1677298119@qq.com, [b] jiajiajiang@tech.edu.cn

Abstract. Polymerization reaction is a strong exothermic reaction that is prone to thermal runaway accidents. To prevent thermal runaway accidents, a styrene thermal polymerization reaction model is established by using computational fluid dynamics (CFD). The failure of stirring speed, cooling temperature of cooling jacket and cooling flow rate during the reaction process are simulated to explore the impact of runaway scenarios on reaction temperature rise and hot spot distribution. The results show that under the conditions of stirring speed of 160 r/min, cooling temperature of 155 ℃ and cooling flow rate of 3.2 m/s, the average temperature of the reaction system is lower and there are fewer hot spot areas, which reduces the possibility of thermal runaway accidents. The monitoring point position that best represents the average temperature of the entire reaction system is located at or above the top one-third of the liquid level.

Keywords: Thermal runaway; Styrene polymerization; CFD; Chaos criterion

1. Introduction

In the chemical reaction process, polymerization reaction is a typical strong exothermic reaction, which can easily cause thermal runaway accidents. In daily experimental operations, there are problems such as long cycles, high costs and limited detection methods. Therefore, the method of simulating and analyzing the flow, reaction and transfer behavior inside the reactor through numerical simulation technology is increasingly valued [1]. Milewska et al. experimental research poses great risks. Milewska et al. simulated the development history of thermal runaway in batch and semi batch reactors [2,3]. Jiang et al. used the critical criterion of thermal runaway to determine the most suitable location for temperature monitoring and studied the influence of temperature curves in reactors [4]. Ni et al. investigated the effect of thermal initiation reaction of styrene on bulk polymerization, pointed out the effects of optimal injection rate, injection position and inhibitor dosage on inhibiting thermal runaway of the reaction [5]. Liu et al. established a compartment model and studied the design of inhibition systems with complex dynamic mechanisms and nonideal mixing effects [6]. In the past, most previous studies focused solely on individual parameters. However, in engineering practice, suppressing thermal runaway requires multiple parameters to act simultaneously. Zaldivar et al. proposed a method that only requires temperature monitoring and calculation of system divergence to detect and alarm the initial stage of reaction runaway [7]. This article explores the appropriate stirring speed, cooling temperature and cooling flow rate, providing a theoretical basis for preventing thermal runaway reactions and having certain guiding significance for engineering applications.

2. Model

2.1 Geometric model of reactor

The total height of the reactor is 240mm, the inner diameter is 120mm, the wall thickness is 5mm, and the liquid level is 80mm. The bottom layer is a four blade 45 ° propeller type agitator, with a diameter of 80mm, a width of 15mm and a thickness of 3mm. The diameter of the agitator shaft is 14mm, and the installation height of the agitator is 10mm from the bottom of the reactor.

2.2 Governing equations

Continuity equation, momentum equation, the energy equation and component transport equation can be represented by the following general equations [1]:

$$\frac{\partial(\rho\Phi)}{\partial t}+\frac{\partial(\rho U_i\Phi)}{\partial x_i}=\frac{\partial}{\partial x_i}(\Gamma_\phi\frac{\partial\Phi}{\partial x_i})+S_\phi \tag{1}$$

ϕ is the dependent variable, ρ is the fluid density, t is the time, Ui is the fluid velocity in the x, y, z direction, Γϕ is the general diffusion coefficient and Sϕ is the source item.

2.3 Geometric model of reactor

Chaos criterion is defined it as the trace of a Jacobian matrix [2-3]:

$$J=\begin{bmatrix} j_{11} & j_{12} \\ j_{21} & j_{22} \end{bmatrix}=\begin{bmatrix} \frac{\partial(\partial\xi/\partial t)}{\partial\xi} & \frac{\partial(\partial\xi/\partial t)}{\partial T} \\ \frac{\partial(\partial T/\partial t)}{\partial\xi} & \frac{\partial(\partial T/\partial t)}{\partial T} \end{bmatrix} \tag{1}$$

In the formula, T is the reactor temperature and ξ is the conversion degree rate of the reactants. which can be simplified as:

$$DIV=j_{11}+j_{22} \tag{2}$$

3. Results analysis

3.1 Mixing failure situation

In the process of styrene polymerization, the stirring effect of the impeller can have a certain impact on the convective heat transfer, system temperature distribution and hot spot area distribution of the reaction system. Therefore, the stirring failure during the styrene thermal polymerization reaction process is simulated, considering the temperature rise and reaction failure time of the reaction system under different operating conditions at stirring speeds of 160r/min, 120r/min, 80r/min, 40r/min and 0r/min.

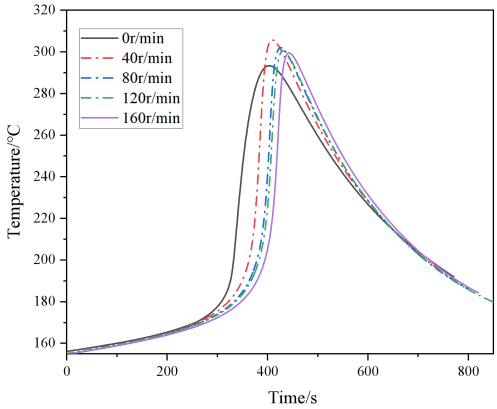

Fig.1 Time-volume average temperature curve for scenario of stirring out of control

Table 1. Effects of stirring rate on runaway time and temperature

Speed/ r·min^{-1}	Time corresponding to the highest reaction temperature /s	Maximum reaction temperature /°C
160	434.10	299.45
120	431.25	300.43
80	426.45	302.05
40	409.60	305.67
0	402.07	293.33

Fig. 1 shows the temperature rise curve and Table 1 shows the data of stirring speed corresponding to the time and temperature. When the stirring speed is 0 r/min, the average temperature rises rapidly to 293.33 °C and the corresponding failure time is 402.07 s. As the stirring speed increases from 40 r/min to 160 r/min, the highest temperature decreases from 305.67 ℃ to 299.45 ℃ and the time also extends from 409.60 s to 434.10 s. This indicates that an increase in stirring speed can reduce the risk of thermal runaway in the reaction system and also prolonging the aging time of the system.

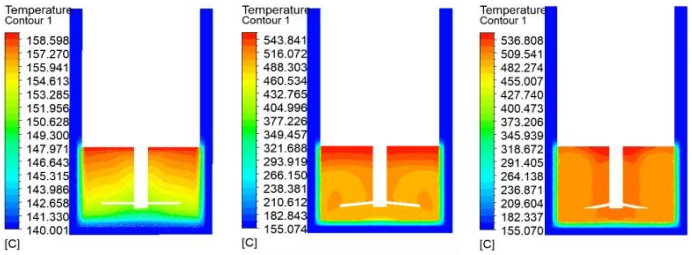

(a) 0 rad/min (b) 80 rad/min (c) 160 rad/min

Fig. 2 Predicted temperature distribution

Fig. 2 shows that as the stirring blade continues to stir, the high-temperature area gradually moves towards the top of the reactor, hot spot area is formed. The laminar flow state appears in the reactor and remains unchanged from 340 s to 640 s. As the stirring speed increases, the laminar flow state inside the reaction system gradually changes, the effect is relatively better at a speed of 160 r/min.

3.2 Cooling temperature failure situation

The temperature control device often generates a temperature difference of about 3 ℃ due to human operation, but a small temperature difference can bring great changes to the temperature rise of the reaction system in the reactor. Therefore, the failure scenario of cooling temperature is studied, considering the working conditions at cooling temperatures of 150 ℃, 151 ℃, 152 ℃ and 153 ℃.

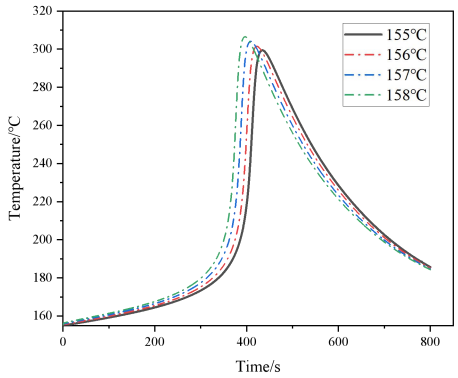

Fig.3 Time vs temperature curves at different cooling temperature

Table 2. Effection of cooling temperature on runaway time and temperature

Cooling temperature/ °C	Time corresponding to the highest reaction temperature /s	Maximum reaction temperature /°C
160	434.10	299.45
120	431.25	300.43
80	426.45	302.05
40	409.60	305.67
0	402.07	293.33

Fig. 3 shows the temperature rise curves of at different cooling temperatures and Table 2 shows the data for the runaway time and temperature. Analysis shows that as the cooling temperature slowly increases, the temperature of the reaction system continues to rise and the corresponding

time also decreases. The temperature of reactor at a cooling temperature of 158 °C increases by 7.2 °C compared to 155 °C and the corresponding runaway time is also advanced by 35.05 s.

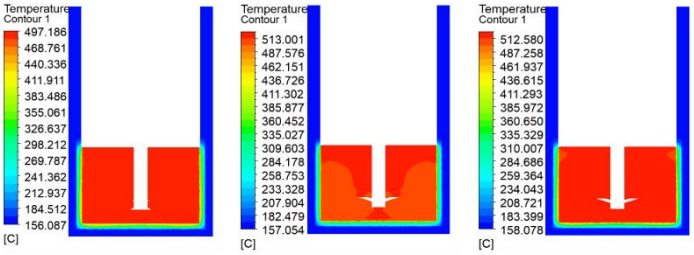

(a) 156 °C (b) 157 °C (c) 158 °C

Fig.4 Temperature distribution at different cooling temperatures

The Y-axis cloud maps of the reactor at different cooling temperatures are shown in Fig. 4. It can be concluded that the change in external temperature of the reactor wall has almost no effect on the distribution of hot spots in the reaction system.

3.3 Cooling flow rate failure situation

Cooling flow rate failure situation is studied further, considering the operating conditions when the inlet flow rates are 3 m/s, 2 m/s, 1 m/s, and 0 m/s.

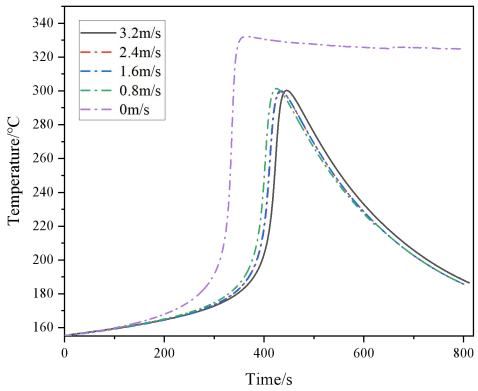

Fig. 5 Time vs temperature curves at different cooling velocity

Table 3. Effection of cooling velocity on runaway time and temperature

Cooling flow rate / °C	Time corresponding to the highest reaction temperature /s	Maximum reaction temperature /°C
3.2	445.55	300.25
2.4	435.30	299.52
1.6	433.95	299.97
0.8	424.65	301.34
0	367.80	332.05

Fig. 5 shows the temperature rise curve in different cooling flow rates and Table 3 shows the data table of time and temperature. When the flow rate is 0 m/s, the temperature of the reactor increases sharply, reaching a high temperature of 332.0 °C at 367.80 s. The failure time at a cooling flow rate of 3.2 m/s is 77.75 s longer than that at 0m/s, which has bought more time for emergency work.

The Y-axis cloud maps of the reaction system at different cooling flow rate are shown in Fig. 6. When the cooling flow rate is 0m/s and the reaction system temperature reaches its highest value in 367.80s, the entire reactor is at its highest temperature, with almost no temperature difference; When the cooling flow rate is 3.2m/s, as the reaction proceeds, the reaction heat zone moves towards the top. The approximate symmetrical and uniform distribution of the temperature field in the reactor.

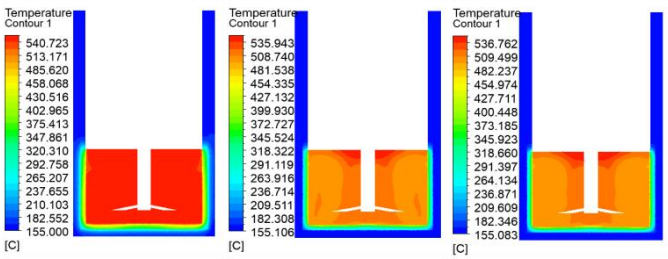

(a) 0 m/s (b) 1.6 m/s (c) 3.2 m/s

Fig. 6 Temperature distribution at different cooling temperatures

3.4 Determine the location of temperature monitoring points

A suitable temperature monitoring point needs to be able to represent the average temperature of the entire reaction system.

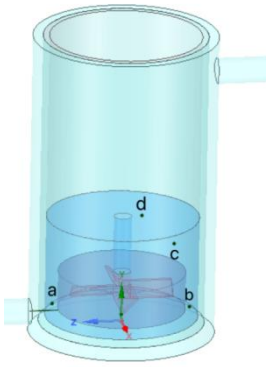

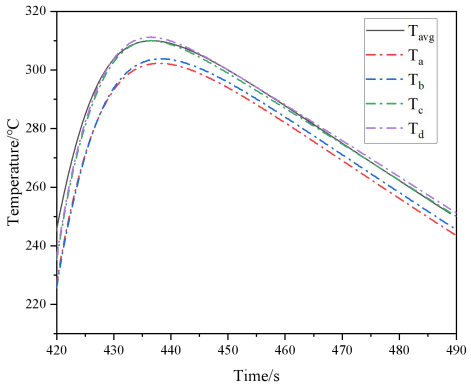

Fig. 7 Monitoring points map Fig. 8 Temperature at different monitoring points

Fig. 7 shows the map of temperature monitoring points. Fig. 8 shows temperature at different monitoring points. In the horizontal direction, as monitoring point a is close to the inlet of the cooling jacket, so Tb>Ta; in the vertical direction, as the hot spot area continuously rises and eventually gathers at the top of the liquid surface, so Td>Tc>Tb. As shown in Fig. 8, the average temperature of the reaction system Tavg ≈ Tc and Td. Therefore, it is preliminarily judged that monitoring points c and d can serve as monitoring points, representing the average temperature of the entire reaction system.

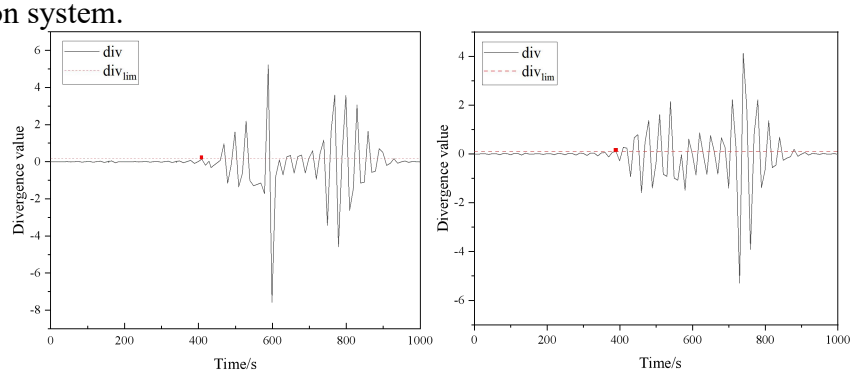

(a) Monitoring point a (b) Monitoring point b

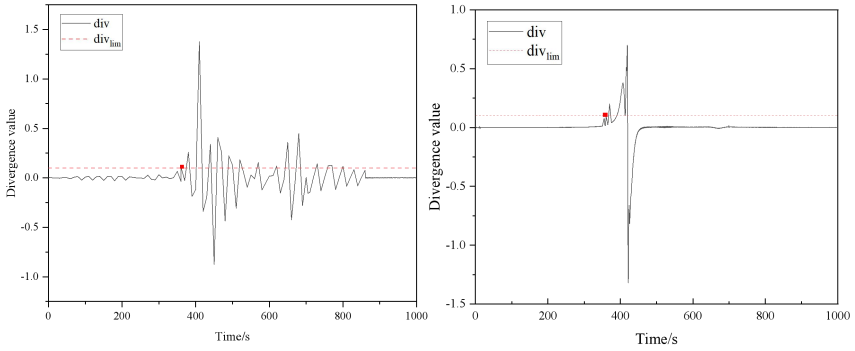

(c) Monitoring point c (d) Monitoring point d

Fig. 9 DIV curves of different temperature monitoring points

Table 4. Time for divlim of a-d

Monitoring point	a	b	c	d
Time to reach div_{lim} /s	408	389.5	360	360.5

In order to avoid false alarms, this article sets a critical line divlim=0.1 as the critical alarm point for thermal runaway. The time corresponding to the earliest point where significant fluctuations occur is used as the critical point for the reaction to run out of control (as shown by the red dots in Fig. 9). According to Table 4, the monitoring point first reaches the critical line of loss of control at 360 s, with a loss of control time Ta>Tb>Tc>Td. So, point c is the most suitable monitoring point, which can timely monitor the occurrence of thermal runaway in the reaction system and reduce the risk.

4. Summary

As the stirring rate increases from 0 r/min to 160 r/min, the high-temperature hot spot area is effectively controlled; The temperature of the reaction system at a cooling temperature of 158 ° C increased by 7.2 ° C compared to 155 ° C and the corresponding runaway time is advanced by 35.05 s. The failure of cooling temperature has almost no effect on the distribution of hot spots; The failure time at 3.2 m/s is 77.75 s longer than that at 0 m/s; The Chaos criterion is used as the alarm standard, the monitoring point position that best represents the average temperature of the entire reaction system is located at or above the top one-third of the liquid level.

References

[1] Kim J.Y., Laurence R.L., The mixing effect on the free radical MMA solution polymerization. Korean Journal of Chemical Engineering, 1998,15(3) : 273-286.

[2] Kim J.Y., Laurence R.L., The mixing effect on the free radical MMA solution polymerization. Korean Journal of Chemical Engineering, 1998,15(3) : 273-286.

[3] Milewska A., Molga E. Safety aspects in modelling and operating of batch and semibatch stirred tank chemical reactors. Chemical Engineering Research & Design 2010, 88, 304–319.

[4] Jiang J., Yang J., Jiang J., Pan Y., Yu Y., Zhou D. Numerical simulation of thermal runaway and inhibition process on the thermal polymerization of styrene. Journal Of Loss Prevention In The Process Industries, 2016, 44, 465-473.

[5] Ni L., Cui J., Jiang J., Pan Y., Wu H., Shu C., Wang Z., Mou S., Shi N. Runaway inhibition of styrene polymerization: A simulation study by chaos divergence theory. Process Safety And Environmental Protection, 2020, 135, 294-300.

[6] Nitin H. CFD analysis of micromixing effects on polymerization in tubular low-density polyethylene reactors Chemical Engineering Science, 1999,54(15) : 3233-3242.

[7] Zaldívar J M, Bosch J, Strozzi F, Zbilut J.P. Early warning detection of runaway initiation using non-linear approaches. Communications in Nonlinear Science and Numerical Simulation, 2003, 10(2005):299-311.

[8] Rudniak L., Machniewski P.M., Milewska A., Molga E. CFD modelling of stirred tank chemical reactors: homogeneous and heterogeneous reaction systems. Chemical Engineering Science, 2004, 59, 5233-5239.

[9] Milewska A., Rudniak L., Molga E. CFD modelling and divergence criterion for safety of chemical reactors. Computer Aided Chemical Engineering. 2005, 20, 259–264.

[10] Bosch J., Kerr D.C., Snee T.J., Strozzi F., Zaldívar J.M. Runaway Detection in a Pilot-Plant Facility. Industrial & Engineering Chemistry Research. 2004, 43, 7019-7024.